

# Nanoporous organic/inorganic hybrid materials produced from poly(dimethyl siloxane)

N.S.M. Stevens, M.E. Rezac\*

*Georgia Institute of Technology, School of Chemical Engineering, 778 Atlantic Drive, Atlanta, GA 30332-0100, USA*

Received 15 June 1998; received in revised form 1 September 1998; accepted 10 September 1998

## Abstract

The partial pyrolysis of poly(dimethyl siloxane) is reported. Pyrolysis is completed in a two step process, inert pyrolysis in a nitrogen atmosphere followed by oxidative pyrolysis in air. Treatment temperatures were from 300–400°C for the inert processing and 260–300°C for oxidative treatment. This thermal processing required no solvents or bulky catalysts, whose transport into the matrix is diffusion controlled and thus limit product uniformity. Therefore, high sample uniformity was achieved. Hybrid materials with reduced carbon and hydrogen content and an increased oxygen/silicon ratio resulted. These composites were shown to be stronger than composites reported in the literature with similar elemental compositions, but prepared in such a way as to achieve only limited interphase interaction. At high oxidation temperatures, microporosity developed in the materials. © 1999 Elsevier Science Ltd. All rights reserved.

*Keywords:* PDMS; Silicone rubber; Partial pyrolysis

## 1. Introduction

Polymer composites have an undeniable technical importance and have been widely investigated and employed [1]. The incorporation of an inorganic phase into an organic polymer matrix may serve to increase mechanical strength and provide improvements in other specific properties. Methods for the preparation of these hybrid systems are varied. The simplest is the direct mixing of an organic polymer solution with an inorganic filler. The surface of the filler may be modified to promote good mixing between the two components [2,3]. To be successfully applied to applications which require optical clarity and significant enhancements in strength as compared to the base polymer, the composite systems must be homogeneous. Phase separation is undesirable in that it can result in a degradation of both optical and mechanical properties.

Numerous reports have appeared on the preparation of organic–inorganic hybrid materials via the in situ polymerization of metal alkoxides in organic polymers [4–18]. The properties of the resultant composites are influenced by the system pH, amount of water employed in the casting dope, type of solvent employed, and sample dimensions. Because polymerization of alkoxides relies on the use of a liquid catalyst, diffusion of the catalyst to the sample core is a

limiting factor in the preparation of uniform materials. Additionally, the use of an organic polymer with the ability to hydrogen bond to the inorganic phase can retard phase separation and result in homogeneous systems [19].

Alternatively, low molecular weight polymer chains can be chemically grafted to the alkoxide prior to alkoxide polymerization. This results in increased silica in the composite with an associated increase in material strength while providing a means of stress dissipation through the presence of the polymer. Thus, these materials have strengths which are higher than composites with lower silica contents and are less brittle than purely ceramic materials. These systems rely upon the same alkoxide polymerization as those previously described. Thus, the properties of these materials are also highly system dependent.

One additional approach utilizes the simultaneous polymerization of organic and inorganic molecules [20]. Novak and coworkers have demonstrated that the simultaneous polymerization of cyclic alkenyl monomers and tetramethoxysilane can result in a single phase system with limited shrinkage if the reaction rates of the two components are well matched [20]. This technique relies upon the production of simultaneous interpenetrating networks, wherein both inorganic glass and polymer formation occur concurrently. Shrinkage issues are minimized by the complete elimination of solvents from the polymerization system. Thus, the process is essentially one of bulk polymerization.

\* Corresponding author.

*E-mail address:* mary.rezac@che.gatech.edu (M.E. Rezac)

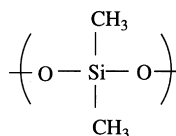


Fig. 1. Schematic of Poly(dimethyl siloxane).

Each of these techniques relies upon the mixing of an inorganic and an organic component in such a way as to maintain homogeneity. While there are certainly reports of how this might be successfully achieved, by the nature of the chemicals employed, it is often a thermodynamically unfavorable operation. In this report, we present an alternative technique for the formation of hybrid organic/inorganic materials. A polymeric material with an inorganic backbone undergoes a partial pyrolysis process which results in a material whose properties are intermediate between those of the initial polymer and those of the inorganic component.

This paper details the processes employed during the partial pyrolysis process and the chemical and mechanical properties of the resulting materials. Poly(dimethyl siloxane) or PDMS has been employed as the model precursor. PDMS is of interest because it is optically clear, readily film forming, inexpensive, and a great deal is known about the thermal and oxidative degradation process of this material [21–33]. Further, PDMS has been approved by the FDA for use in humans. Unfortunately, in the virgin state, PDMS is a rather low-strength rubber and its application is limited by this fact. This manuscript describes the chemical and mechanical changes which result upon a partial pyrolysis process.

## 2. Experimental

### 2.1. Materials

Poly(dimethyl siloxane), RTV 615, was obtained from GE<sup>®</sup> Plastics. The structure of PDMS is shown in Fig. 1. This material crosslinks at room temperature following the combination of a prepolymer and a crosslinking agent. A weight ratio of 10 parts polymer to one part crosslinking agent was employed for all films.

Homogeneous PDMS samples were prepared by pouring a 14.0% by weight silicone rubber/toluene solution into casting dishes. Casting dishes were placed in a toluene

enriched atmosphere to minimize the rate of evaporation. Following 48 h drying, the samples were removed from the casting dishes and the toluene environment. Samples were dried for an additional 72 h in 25°C air and 1 h in a vacuum oven at 100°C. Following drying, samples thicknesses ranged from 20 to 150 μm.

Toluene (reagent grade, J. T. Baker, 99.99%) was used for silicone rubber solutions without further purification. Methanol (reagent grade, Fisher 99.9%) was used for sorption studies without further purification. Nitrogen (minimum purity 99.9%) was obtained from Air Products and South East Air Gas and used as received. Air was compressed from the atmosphere through the use of an oil primed, ring compressor.

### 2.2. Partial pyrolysis

Samples were placed on a wire rack and then into a stainless steel pyrolysis vessel. This vessel was maintained in an oven capable of regulating the system temperature to within  $\pm 0.2^\circ\text{C}$ . Nitrogen was purged through the vessel and past the sample at 5 ml/min. Under nitrogen purge, the oven was heated from room temperature to  $T_p$  (purge gas temperature) at a heating rate of  $6.25^\circ\text{C}/\text{min}$ . Samples were held at  $T_p$  for 5 h, beginning as the oven was turned on. The oven temperature was then lowered to the oxidative temperature,  $T_o$ , and allowed to cool for 1.5 h. At this time, the nitrogen flow was shut off and air flow was directed through the pyrolysis vessel. After additional 5 h, the oven was turned off and allowed to cool to room temperature under air flow. Experimental parameters can be seen in Table 1.

### 2.3. NMR

A Bruker DSX-400 was employed for solid state  $^{29}\text{Si}$  measurement. A high speed MAS (magic angle spinning) probe at a rotational frequency of 10 000 Hz was used. A single pulse  $^{29}\text{Si}$  excitation frequency of 79.43 MHz was employed with a pulse length of 3 ms. The peak at  $-19.5$  ppm was referenced as the dimethylsiloxane peak [12].

### 2.4. Infrared studies

A Vector 22 infrared system was used for infrared studies. The modified samples were ground to powder and formed into pellets with the incorporation of potassium bromide. Thirty-two scans were averaged to form a single spectra.

### 2.5. Mechanical properties

A Seiko DMS 210 was used to measure modulus and  $\tan \delta$  of the pyrolyzed silicone rubber samples. Scans were made at a frequency of 1 Hz over a temperature range of  $-140^\circ\text{C}$  to  $150^\circ\text{C}$  in a nitrogen environment.

Stress–strain measurements of these samples were tested using an Endura-Tec Microtester. This microtester is

Table 1  
Pyrolysis Experimental Parameters.

Factor	Values
Purge Gas	Nitrogen
$T_p$ , Purge Gas Temperature ( $^\circ\text{C}$ )	200, 250, 300, 350, 400
$T_o$ , Oxidative Temperature ( $^\circ\text{C}$ )	260, 280, 300
Purge Gas Time	5 h
Air Time	5 h
Gas Flow Rate	5 ml/sec

Table 2  
Elemental Analysis of virgin PDMS and partially pyrolyzed PDMS by mass percentage

	Mass Losses			Elemental Composition (Mass %)			
	MLp (%)	MLo (%)	Oxidative reaction exotherm (J/g)	C (%)	H (%)	Si (%)	O (%)
PDMS (calculated from Fig. 1)	N/A	N/A	N/A	32.4	8.1	37.9	21.6
PDMS (experimental)	N/A	N/A	N/A	30	7.7	—	—
$T_p = 200^\circ\text{C}$ , $T_o = 260^\circ\text{C}$	< 0.1	2.5	-570	25.4	6.4	36.2	32.0
$T_p = 400^\circ\text{C}$ , $T_o = 260^\circ\text{C}$	22.5	0.1	-80	23	5.9	—	—
$T_p = 400^\circ\text{C}$ , $T_o = 280^\circ\text{C}$	22.5	1.2	-1400	19	5.4	—	—
$T_p = 400^\circ\text{C}$ , $T_o = 300^\circ\text{C}$	22.5	3.0	-2200	14.0, 11.1	4.4, 4.2	—, 41.6	—, 43.5

designed for a maximum load of 50 lbs. The procedure employed was consistent with ASTM D882. A ruler was used to measure the initial separation between the grips, and a thick, aluminum bar was used to measure machine compliance prior to sample testing.

### 2.6. Sorption

The gravimetric method was employed to measure both sorption and desorption of methanol into the partially pyrolyzed samples. A Cahn D-200 balance was used for sorption studies. Sorption was measured at  $30.0 \pm 0.1^\circ\text{C}$ . Details of this equipment have been provided [34]. Sorption and desorption measurements were carried out for a minimum of 20 times the half time.

### 2.7. Thermal analysis

A Setaram TG-DSC 111 was used for simultaneous thermogravimetric and differential scanning calorimetric analysis. The heating rate and cooling rate of the instrument were set to  $6.25^\circ\text{C}/\text{min}$  and  $3.5^\circ\text{C}/\text{min}$ , respectively, so as to mimic the oven behavior during sample preparation. The mass losses reported were calculated as follows:

$$\text{MLp} = \frac{M_i - M_p}{M_i} \times 100\% \quad (1)$$

$$\text{MLo} = \frac{M_p - M_o}{M_p} \times 100\% \quad (2)$$

where  $M_i$  is the mass loss prior to treatment;  $M_p$  is the mass loss following 5 h of pyrolysis at  $T_p$ ; and  $M_o$  is the mass loss following 5 h of oxidation at  $T_o$ .

## 3. Results and discussion

The purpose of this research was to explore the possibility of forming inorganic components which are uniformly distributed within and covalently bound to an organic matrix. The use of an in-situ processing technique to form such composites is explored. Alternative production methods include the admixing of inorganic fillers in an organic matrix and the in-situ polymerization of metal alkoxides in

organic polymers. In the following sections, the properties of the materials produced in the current study will be detailed. Where appropriate, the properties of the current materials will be compared to hybrid materials produced using one of the two techniques described.

### 3.1. Sample appearance

All samples prepared with an oxidative temperature of  $260^\circ\text{C}$  or less were optically clear. Samples prepared with higher oxidative temperatures ranged from clear to translucent. Some of the samples treated at  $T_o = 300^\circ\text{C}$  formed brittle films which crumbled into powders under load. Inspection of the sample fragments indicated that cracks present in the sample appear to have provided a mechanism for light diffraction. Samples which were sufficiently small to be crack free were optically clear.

Within experimental detection capacity, the optical, chemical and mechanical properties were independent of the location within the material sampled or the original material geometry.

### 3.2. Changes in chemical composition

Chemical characterization of the PDMS samples was made before and after the partial pyrolysis process was completed. Characterization included elemental analysis of the resultant solids, infrared analysis, and solid state nuclear magnetic resonance analysis. Further, the mass loss upon processing was recorded.

Partial pyrolysis followed by oxidative treatment results in a chemical structure with a decrease in the molecular level of carbon and hydrogen as is detailed in Table 2. As the pyrolysis and oxidation temperatures increase, the carbon content decreases. Although the exact reaction products were not analyzed in this study, the resultant composition is consistent with a decrease in the relative ratio of methyl to  $-\text{Si}-\text{O}-$  groups. Nevertheless, a significant fraction of the initial methyl groups remains following processing at the conditions reported. Thus, the pyrolysis may be viewed as incomplete, or "partial".

The mass loss of the samples increases with increases in pyrolysis and oxidation temperature. For the conditions investigated, the majority of the decomposition occurred

Table 3  
Analytical fingerprint of polysiloxanes: NMR resonances and FTIR wave-numbers

NMR peak location of polysiloxanes [36,37]		
Notation	Chemical Structure	Chemical Shift
M	$(\text{CH}_3)_3\text{SiO}_{0.5}$	7 to 9 ppm
D	$(\text{CH}_3)_2\text{Si}(\text{O}_{0.5})_2$	- 19 to - 23 ppm
Q	$(\text{CH}_3)\text{Si}(\text{O}_{0.5})_3$	- 65 to - 72 ppm
T	$\text{Si}(\text{O}_{0.5})_4$	- 103 to - 113 ppm
D <sup>OH</sup>	$(\text{CH}_3)(\text{OH})\text{Si}(\text{O}_{0.5})_2$	- 55 to - 58 ppm
D <sup>OMe</sup>	$(\text{CH}_3)(\text{OCH}_3)\text{Si}(\text{O}_{0.5})_2$	- 56 to - 58 ppm
FTIR: Selected vibrational frequencies for siloxane groups [38,39]		
Group	Wavenumber ( $\text{cm}^{-1}$ )	
O–Si–O Asymmetric Stretch	1130 to 1000	
Si–CH <sub>3</sub> Symmetric Deformation	1280 to 1240	
Si–CH <sub>3</sub> Asymmetric Deformation	1460 to 1375	
Si–CH <sub>3</sub> Asymmetric Rock	870 to 750	
Si–C Stretch	3650 to 3580	
O–H Due to H <sub>2</sub> O (free)	3550 to 3200	
O–H Due to H <sub>2</sub> O (H-bonded)	3700 to 3200	
Si–OH Stretch	1100–830	
Si–O Stretch		

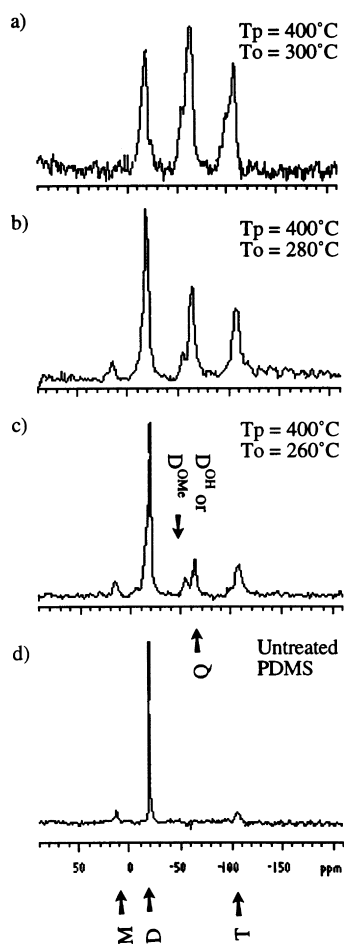


Fig. 2. Single pulse  $^{29}\text{Si}$  MAS data for samples treated at a pyrolysis temperature of  $400^\circ\text{C}$  and oxidation temperatures of (a)  $300^\circ\text{C}$ , (b)  $280^\circ\text{C}$  and (c)  $260^\circ\text{C}$ ; (d) untreated PDMS.

during the inert pyrolysis stage. Nevertheless, the reaction exotherm upon oxidation increased markedly as the temperature of oxidation increased from  $260^\circ\text{C}$  to  $280^\circ\text{C}$ . A smaller increase occurred as the oxidative temperature was elevated to  $300^\circ\text{C}$ .

In order to provide an approximate comparison between these materials and those prepared by mixing silica and PDMS phases, the effective silica content in the materials has been calculated from elemental analysis. These calculations require that several assumptions be made. The assumptions made when completing these calculations include:

1. Carbon contributes only to methyl groups.
2. The number of polymeric chain ends is negligible
3. Oxygen contributes only to siloxane repeat units, silica repeat units ( $\text{SiO}_2$ ), and hydroxyl groups.
4. The siloxane repeat units are separable from the silica units.

The calculated weight percent of the silica content in the partially pyrolyzed PDMS samples formed in this study is between 14%, for samples treated at the lowest temperatures ( $T_p = 200^\circ\text{C}$ ,  $T_o = 260^\circ\text{C}$ ), and 42%, for samples treated at the highest temperatures ( $T_p = 400^\circ\text{C}$ ,  $T_o = 260^\circ\text{C}$ ).

It is clear from the data presented in Table 2 that some

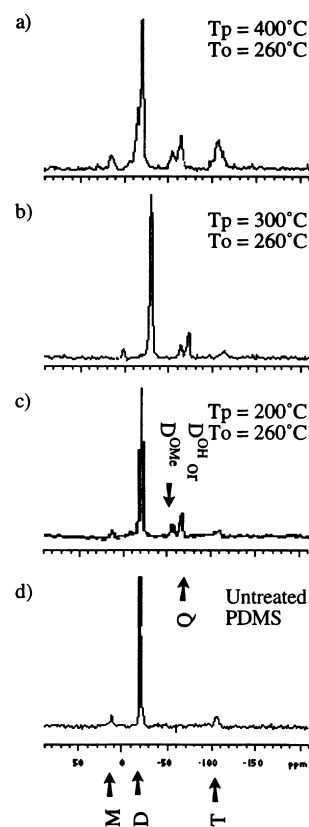


Fig. 3. Single pulse  $^{29}\text{Si}$  MAS data for samples treated at an oxidative temperature of  $260^\circ\text{C}$  and pyrolysis temperatures of (a)  $400^\circ\text{C}$ , (b)  $300^\circ\text{C}$  and (c)  $200^\circ\text{C}$ ; (d) untreated PDMS.

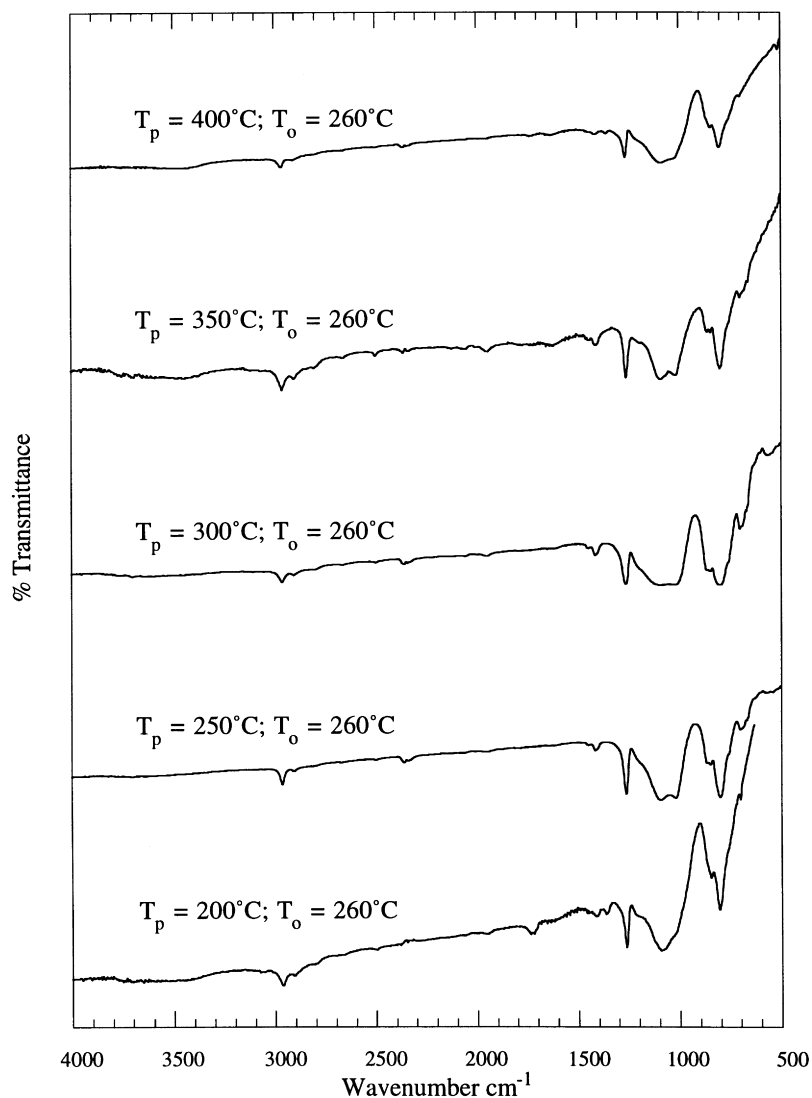


Fig. 4. IR of modified samples treated at varying purge gas temperatures and an oxidative temperature of 260°C.

methyl groups are eliminated from the virgin PDMS and that oxygen is incorporated in the matrix. Insight into the chemical nature of the final product is provided by solid state NMR analysis and FTIR analysis. The terminology commonly associated with the analysis of polysiloxanes by NMR and their resonances are provided in Table 3 for reference. Also provided are the wavenumbers for vibrations of interest for FTIR analysis of polysiloxanes. Quantitative data from single-pulse MAS  $^{29}\text{Si}$  spectra (as measured here) is not reliable, but qualitative analysis is possible [35]. The numerical concentrations of each component have, therefore, not been calculated. A discussion of the relative presence of the components follows.

NMR spectra for samples partially pyrolyzed at a temperature of 400°C and oxidized at temperatures of 260°C, 280°C, and 300°C are provided in Fig. 2. As the oxidation temperature increases, the ratios of tri-substituted and tetra-substituted silicon groups to the dimethylsiloxane peak increase. The relative intensity of the D peak

decreases. Therefore, as the oxidation temperature increases, the number of methyl groups attached to the silicon–oxygen backbone decreases and the amount of cross-linking, as exhibited by the increase in Q and T groups, increases.

The change in peak intensities is not as dramatic for samples treated at a constant oxidation temperature of 260°C and purge gas temperatures of 200°C, 300°C, and 400°C as detailed in Fig. 3. At the lowest treatment temperature (200°C),  $(\text{CH}_3)\text{Si}(\text{O}_{0.5})_3$  bonding is observed (peaks appear at  $-56$  and  $-68$  ppm). The relative content of the tetra-substituted silicon ( $-110$  ppm) increases as the pyrolysis temperature increases. Nevertheless, the D peak [ $(\text{CH}_3)_2\text{Si}(\text{O}_{0.5})_2$ , at  $-23$  ppm] remains dominant, indicating that few methyl groups are lost. This, when compared to Fig. 2, demonstrates that the majority of chemical changes occur at greater oxidation temperatures.

Infrared spectra of modified samples are shown in Figs. 4 and 5. All show the anticipated peak for the O–Si–O

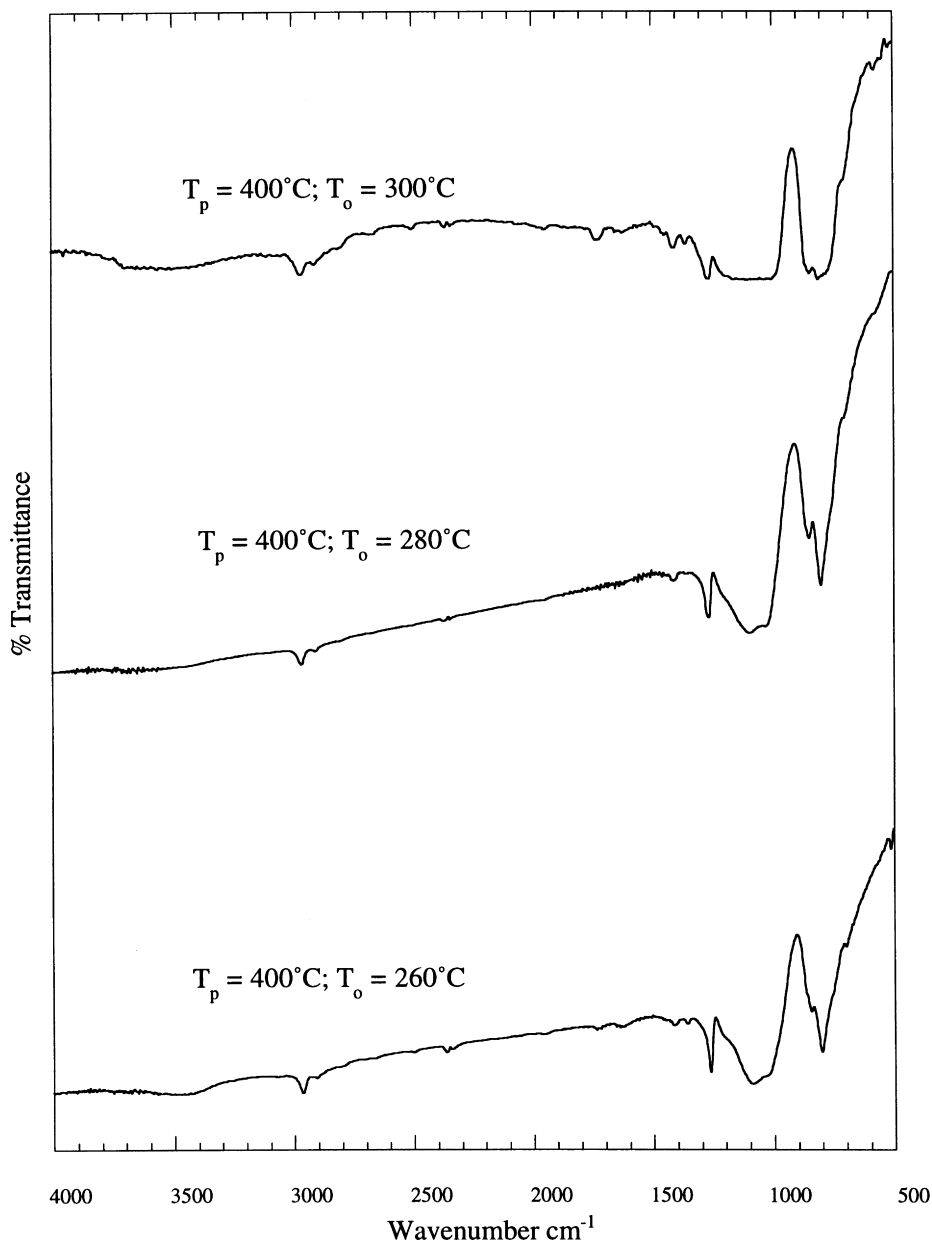


Figure 5. IR of modified samples treated at a purge gas temperature of 400°C and varying oxidative temperatures.

asymmetric stretch from 1200 to 1000  $\text{cm}^{-1}$ . Additionally, methyl groups contribute in the peaks at about 2950  $\text{cm}^{-1}$ , 800  $\text{cm}^{-1}$ , 1280  $\text{cm}^{-1}$ , and 1430  $\text{cm}^{-1}$ .

There are not dramatic differences in the IR spectra of samples treated over the entire range of conditions evaluated here. All samples indicate the presence of O–Si–O and –CH<sub>3</sub> groups. Thus, while NMR has confirmed that the relative presence of the Q, T, and D peaks changes with processing conditions, IR indicates that all conditions result in the same types of bonding, just to a different extent.

The shoulder at approximately  $-56$  ppm in Fig. 2 could represent either D<sup>OH</sup> or D<sup>OMe</sup>. The hydroxyl side group has been shown to be an oxidative product of silicone rubber

and is the likely source of this peak. IR spectra indicate the presence of a broad band from 3800 to 3300  $\text{cm}^{-1}$ . This is clearly demonstrated in Fig. 6, which details the high wavenumber portion of the spectrum for the  $T_p = 400^\circ\text{C}$ ,  $T_o = 300^\circ\text{C}$  sample as an illustrative example. The broad band, which is indicative of hydroxyl bonding, occurs at wavenumbers that are greater than those expected for water. Thus, one can infer that Si–OH groups are present in the modified samples [38]. The shoulder, present at 850  $\text{cm}^{-1}$ , is characteristic of Si–OH groups and adds weight to this conclusion. Regardless, these shoulders are quite small and are not expected to play a major role in the material behavior.

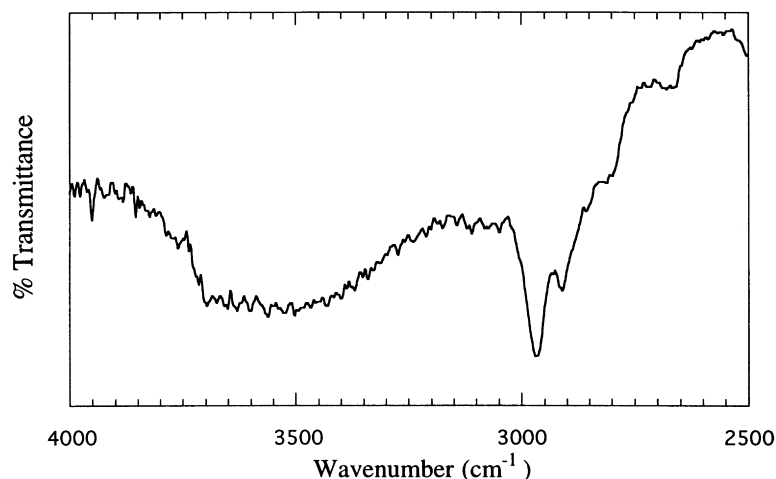


Fig. 6. Enhancement of IR spectrum of sample treated at an inert gas temperature of 400°C and an oxidative temperature of 300°C.

### 3.3. Mechanical properties

As crosslinking increases, polymer segments lose mobility and transition temperatures increase. Crosslinking effects are seen using dynamic mechanical analysis, or, more precisely, by viewing the loss factor,  $\tan \delta$ , as a function of temperature. The loss factor shows a sharp peak for amorphous, unoriented material and a broad, flat peak for crystalline, highly crosslinked, or oriented material [40]. As crosslinking increases and segments lose mobility, the magnitude of  $\tan \delta$  decreases and peaks broaden.

Results of  $\tan \delta$  measurements of the samples are summarized in Table 4. Samples prepared with  $T_p$  greater than 300°C were too brittle for measurement. As purge gas temperatures increase, the intensity of the  $\tan \delta$  peaks decrease and the peaks shift to higher onset temperatures, representing a loss in sample mobility.

The trends observed are consistent with the results achieved when silicone rubber was added to tetraethoxysilane (TEOS) prior to a sol-gel processing [10]. As the concentration of silica (formed from the condensation of TEOS) increased,  $\tan \delta$  peaks broadened and shortened, and the transition temperature shifted to a higher value. Storage modulus also increased as the percent TEOS was increased [10]. Storage moduli for the partially pyrolyzed PDMS samples considered here appeared to follow this

trend. All materials had storage moduli which were statistically equivalent. All values of moduli at the low temperature plateau ( $-150^\circ\text{C}$ ) fell within the range of  $9 \times 10^9$ – $1.7 \times 10^{10}$  Pa.

The elastic moduli follow the same trend of increasing strength with increasing pyrolysis temperatures (see Table 5). Also provided in Table 5, the moduli of the present materials are compared to those of materials prepared by (a) admixing silica particles with PDMS, (b) the condensation of TEOS in a PDMS matrix, and (c) the incorporation of PDMS in a TEOS matrix.

At approximately equivalent silica contents, the composites of the present study are an order of magnitude stronger than those prepared by the admixing of silica particles with PDMS. Composites prepared by the in situ consolidation of TEOS in a PDMS matrix are slightly stronger than those prepared by simple admixing. This increase in strength is believed to be due to a reduction in the particle size of the inorganic phase (TEOS particles are smaller than admixed silica). Nevertheless, PDMS composites prepared by admixing silica or by TEOS consolidation are known to have limited compatibility and do not readily dissipate energy at phase interfaces [17]. When these systems are compared to the hybrid materials prepared in the present study, it is clear that at equivalent silica loadings, the materials prepared by partial pyrolysis are significantly stronger. This supports

Table 4  
Dynamic mechanical behavior of partially pyrolyzed PDMS;  $\tan \delta$  transitions.

Material	Peak 1 (°C)	Magnitude of Peak	Peak Width at 1/2 Height(°C)	Peak 2 (°C)	Magnitude of Peak	Peak Width at 1/2 Height (°C)
Silicone Rubber	-116( $T_g$ )	0.39	19	-48( $T_m$ )	0.20	8
$T_p = 200^\circ\text{C}$ , $T_o = 260^\circ\text{C}$	-85	0.20	88 <sup>a</sup>	—	—	—
$T_p = 250^\circ\text{C}$ , $T_o = 260^\circ\text{C}$	-89	0.17	54	-45	0.16	94
$T_p = 300^\circ\text{C}$ , $T_o = 260^\circ\text{C}$	-54	0.16	92	-31	0.17	82

<sup>a</sup> All samples, except that pyrolyzed at 200°C, showed two maxima in the  $\tan \delta$  plots. Originally, the peak at the lower temperature resulted from the glass transition and the peak at the higher temperature resulted from crystal melting. The location of these peaks in the virgin PDMS is in good agreement with prior reports [41].

Table 5  
Comparison of mechanical properties of samples formed in this study and those formed in previous studies

Sample	Weight% Silica	Elastic Modulus (N/mm <sup>2</sup> )	Reference
Silicone Rubber	0	0.481	4
Silica Filled Silicone	10	0.62	11
Silica Filled Silicone	20	0.85	11
Silicone Filled via TEOS Precipitation	14.6	3.99	4
$T_p = 200^\circ\text{C}, T_o = 260^\circ\text{C}$	14	$11 \pm 1$	
$T_p = 250^\circ\text{C}, T_o = 260^\circ\text{C}$		$14.5 \pm 0.1$	
$T_p = 350^\circ\text{C}, T_o = 260^\circ\text{C}$	21–26	$20 \pm 1$	
TEOS Modified with PDMS	72	192	42

the physical picture of an inorganic phase covalently bound to an organic matrix which readily dissipates stresses.

Finally, the elastic moduli of the partially pyrolyzed materials are approximately an order of magnitude lower than those prepared by the incorporation of PDMS in a TEOS matrix. While these latter materials may also be phase separated [42], the dramatic increase in silica content results in a higher moduli value.

#### 3.4. Morphology changes resulting from the formation of organic/inorganic material

The change in material characteristics can also be seen by

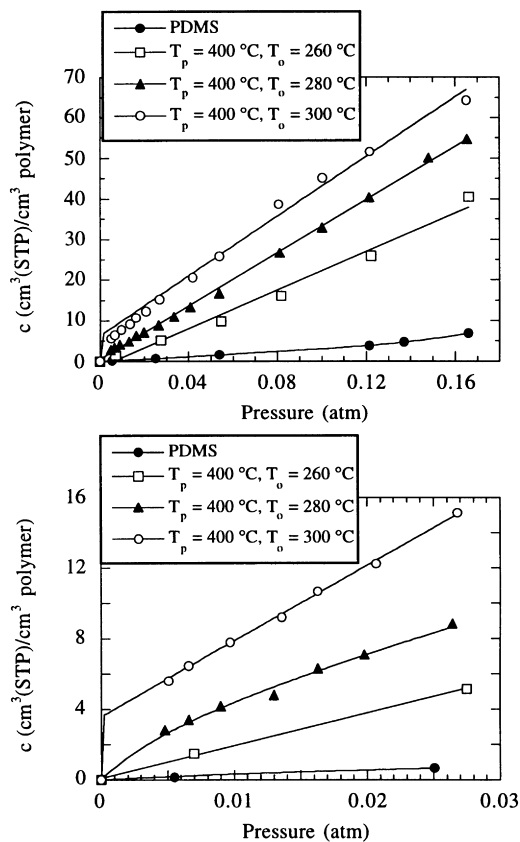


Fig. 7. Sorption of methanol at 30°C into PDMS and partially pyrolyzed PDMS.

changes in the manner in which the material sorbs vapors. Rubbers and ceramics show different behaviors: rubbers tend to absorb and follow Henry's Law at low concentrations of sorbant, while ceramics tend to adsorb resulting in a Langmuir isotherm. If a sample exhibits both rubbery and ceramic behavior, a combination of the two isotherms results and sorptive behavior will follow the dual-mode sorption model:

$$c = k_D p + \frac{c'_H b p}{1 + b p} \quad (3)$$

where  $c$  is the concentration of sorbant in the sample;  $k_D$  is the Henry's law constant;  $p$  is the pressure of the sorbant in the material;  $c'_H$  is the 'hole saturation' constant; and  $b$  is the 'hole affinity' constant [43]. We have fit the data for sorption of methanol into microporous materials using this equation.

Sorption of methanol into the treated samples demonstrates a change in material morphology as is detailed in Fig. 7. As the treatment temperature increases, sorption isotherms no longer follow Henry's law, but begin to follow the dual-mode mechanism. The dual-mode constants for the samples presented in Fig. 7(a) are reported in Table 6. A magnified view of the data at very low activities is shown in Fig. 7(b). Analysis of this figure indicates that the materials oxidized at 280°C and 300°C exhibit dual-mode type behavior. In contrast, the material oxidized at 260°C and the pure PDMS material are best fit using only the first term of Eq. (3). Thus, these materials are characterized by a Henry's law type sorption only. The change in sorption isotherms represents the partial transition of material morphology from a rubbery material towards that of a microporous ceramic.

Analysis of the data presented in Table 6 and Fig. 7 indicates that a transformation from a purely rubbery morphology to one of a mixed matrix form takes place in these materials upon partial pyrolysis. The data presented in Table 6 fall in two categories. The PDMS material and the material oxidized at 260°C have hole affinity constants near zero. Therefore, they behave as if they have no microvoids present in the matrix and are well described by a Henry's Law type isotherm. In contrast, the materials oxidized at 280°C and 300°C have hole affinity constants and hole



Table 6

Dual-mode constants for the partially pyrolyzed samples. Calculated by fitting sorption isotherms shown in Fig. 7 with Eq. (3)

Sample	$k_D(\text{cm}^3(\text{STP})/\text{cm}^3 \text{ polymer atm})$	$c'_H (\text{cm}^3(\text{STP})/\text{cm}^3 \text{ polymer})$	$b (\text{atm}^{-1})$
PDMS	26	—	—
$T_p = 400, T_o = 260$	175	0.3	0.001
$T_p = 400, T_o = 280$	270	17	0.166
$T_p = 400, T_o = 300$	301	18	0.032

saturation constants which are non-zero. Thus, these materials exhibit some microporous-type behavior. Further analysis indicates that the Henry's law constant,  $k_D$ , increases as the pyrolysis and oxidation temperature increase. The value increases significantly when pure PDMS is treated at a pyrolysis temperature of 400°C and an oxidation temperature of 260°C. Further increases in the oxidation temperature continue to increase this value.

The behavior demonstrated by these materials can be rationalized with the following physical picture. Pure PDMS is an hydrophobic, rubbery polymer. This material has a moderate affinity for methanol vapors [34]. Yet, the hydrophobic nature of the polymer backbone limits the amount of methanol which is sorbed. Following pyrolysis at  $T_p = 400^\circ\text{C}$  and  $T_o = 260^\circ\text{C}$ , the relative concentration of hydrophobic methyl groups in the polymer matrix is reduced (see Table 2). This reduction in methyl groups is associated with an increase in the equilibrium sorption of methanol in the polymer because of a reduction in the hydrophobicity of the material. Further increases in the oxidation temperature results in (i) a reduction the methyl group concentration (and an associated reduction in the hydrophobicity of the polymer matrix and an increase in the methanol Henry's law constant), and (ii) the production of a microporous material with significant increase in the equilibrium sorption because of a non-zero contribution from sorption in holes.

The presence of microporosity in these samples has been confirmed by BET measurements and by evaluation of the mechanism of transport of gases through the matrix. BET analysis indicated that pores with an average diameter of less than 40 Å resulted from pyrolysis at 400°C and oxidation at 300°C. Analysis of the transport of gases through the matrix has been reported [44]. Transport analysis indicates that samples pyrolyzed with an oxidation temperature of 260°C and a pyrolysis temperature of  $\leq 380^\circ\text{C}$  were nonporous in nature. Samples prepared with pyrolysis temperatures of 380°C or 400°C and an oxidation temperature of 280°C or 300°C were porous with surface diffusion control [44], indicative of pores of less than 40 Å diameter.

#### 4. Conclusions

Composites have been formed from the partial pyrolysis and subsequent oxidation of silicone rubber. Pyrolysis is accompanied by weight loss of up to 25%. Elemental

analysis indicates that this loss is predominantly due to the loss of carbon and hydrogen. Oxygen has been shown to be incorporated into the matrix upon oxidative treatment. Consequently, the relative oxygen/silicon ratio increases as does the oxidation state of the silicon (as shown by NMR). Change in oxidation temperature has the most dramatic impact on the amount of crosslinking. Dynamic mechanical analysis shows that as the pyrolysis temperature increases,  $\tan \delta$  peaks show that crosslinking increases and storage modulus increases.

This oxidative "crosslinking" provides covalent bond formation between regions of high  $-\text{Si}-\text{O}-$  concentration and regions of the virgin PDMS. This covalent bonding results in an increase in mechanical properties with an increase in both pyrolysis and oxidation temperatures. The elastic moduli of the current materials are markedly higher than those of organic/inorganic composites prepared either by the admixing of silica particles in PDMS or the consolidation of TEOS in PMDS at equivalent silica loadings.

A marked difference between the hybrid organic/inorganic materials produced here and those reported in the literature is that pores are created in the present materials through the partial pyrolysis and oxidation process. Porosity is not a necessary outcome of any of the alternative technologies and has not been reported for those systems. Controlled porosity may be beneficial for applications of silicones as sensors or as membranes. Indeed, we are examining the potential applicability of these materials for the above applications.

Partial pyrolysis may offer an easily processable alternative to a silica filled silicone rubber. Further, the treatments employed are bulk, thermal processes. They require no additional solvents or catalysts to achieve desirable properties. Therefore, sample homogeneity should be high.

#### Acknowledgements

Acknowledgment is made to the donors of the Petroleum Research Fund, administered by the American Chemical Society, for partial support of this research. N. S. M. Stevens acknowledges the Texaco Foundation for partial financial support. The authors acknowledge Dr. Johannes Leisen, Mr. Gary Sturgill, and Dr. Richard Neu and his research group for assistance with NMR, IR, and elastic moduli measurements, respectively.

## References

- [1] Manson JA, Sperling LH. *Polymer Blends and Composites*. New York: Plenum Press, 1976.
- [2] Plueddemann EP. *Silane Coupling Agents*. New York: Plenum Press, 1982.
- [3] Arkels B. *Chemtech* 1977;7:766.
- [4] Mark JE, Jiang CY, Tang MY. *Macromolecules* 1984;17:2613.
- [5] Wilkes GL, Orlor B, Huang H-H. *Polymer Preprints* 1985;26(2):300.
- [6] Mark JE, Ning Y-P, Jiang C-Y, Tang M-Y, Roth WC. *Polymer* 1985;26:2069.
- [7] Tang M-Y, Mark JE. *Polym. Eng. Sci.* 1985;22:29.
- [8] Schmidt H. *J Non-Crystalline Solids* 1985;73:681.
- [9] Ravaine D, Seminel A, Charbouillot Y, Vincens M. *J Non-Crystalline Solids* 1986;82:210.
- [10] Huang H-H, Orlor B, Wilkes GL. *Macromolecules* 1987;20:1322.
- [11] Sun C-C, Mark JE. *Polymer* 1989;30:104.
- [12] Garrido L, Mark JE, Sun CC, Ackerman JL, Chang C. *Macromolecules* 1991;24:4067.
- [13] Nakanishi K, Soga N. *J Non-Crystalline Solids* 1992;139:1.
- [14] Nakanishi K, Soga N. *J Non-Crystalline Solids* 1992;139:14.
- [15] Landry CJT, Coltrain BK, Brady BK. *Polymer* 1992;33:1486.
- [16] Landry CJT, Coltrain BK, Landry MR, Fitzgerald JJ, Long VK. *Macromolecules* 1993;26:3702.
- [17] Silveira KF, Yoshida IVP, Nunes SP. *Polymer* 1995;36:1425.
- [18] Hyeon-Lee J, Guo L, Beaucage G, Macip-Boulis MA, Yang AJM. *J Polym Sci: Part B: Polym Phys* 1996;34:3073.
- [19] Landry CJT, Coltrain BK, Wesson JA, Zumbulyadis N, Lippert JL. *Polymer* 1992;33:1496.
- [20] Ellsworth MW, Novak BM. *J Am Chem Soc* 1991;113:2756–2758.
- [21] Lewis CW. *J Polym Sci* 1958; 33:153.
- [22] Scala LC, Hickam WM. *Ind Eng Chem* 1958;50:1583.
- [23] Nielsen JM. *Adv Chem Ser (Amer Chem Soc)* 1968;85:96.
- [24] Thomas TH, Kendrick TC. *J Polym Sci: Part A-2* 1969;7:537.
- [25] Thomas TH, Kendrick TC. *J Polym Sci: Part A-2* 1970;8:1823.
- [26] Nielsen JM. *J Polym Sci: Symp* 1973;40:189.
- [27] David C. Thermal degradation of polymers. *Degradation of Polymers, Comprehensive Chemical Kinetics*, 14. New York: Elsevier Scientific Publishing Co, 1975 p. 104-107.
- [28] Rabek JF. Oxidative degradation of polymers. *Degradation of Polymers, Comprehensive Chemical Kinetics*, 14. New York: Elsevier Scientific Publishing Co, 1975 p. 456-457.
- [29] Grassie N, Macfarlane IG. *Eur Polym J* 1978;14:875.
- [30] Nielsen JM. *J Appl Polym Sci Appl Polym Symp* 1979;35:223.
- [31] Bannister DJ, Semlyen JA. *Polymer* 1981;22:377.
- [32] Clarson SJ, Semlyen JA. *Polymer* 1986;27:91.
- [33] Ishida H, Dunkers J. *J Appl Polym Sci* 1992;44:1331.
- [34] Rezac ME, John T, Pfromm PH. *J Appl Polym Sci* 1997;65:1983.
- [35] Engelhardt G, Koller H. <sup>29</sup>Si NMR of Inorganic Solids. In: Blumich B, editor. *Solid-State NMR II Inorganic Matter*, New York: Springer-Verlag, 1994 pp. 1-6.
- [36] Beshah K, Mark JE, Ackerman JL, Himstedt A. *J Polym Sci: Part B: Polym Phys* 1986;24:1207.
- [37] Williams EA. NMR Spectroscopy of Organosilicon Compounds. In: Patai S, Rappoport Z, editors. *The Chemistry of Organic Silicon Compounds*, John Wiley & Sons Ltd, 1989 p. 545-547.
- [38] Silverstein RM, Bassler GC, Morrill TC. *Spectrometric Identification of Organic Compounds*. New York: Wiley, 1991.
- [39] Smith AL. *Analysis of Silicones*. New York: Wiley, 1974.
- [40] Ward IM. *Mechanical Properties of Solid Polymers*. New York: Wiley, 1983.
- [41] Brandrup J, Immergut EH. *Polymer Handbook*. New York: Wiley, 1975.
- [42] Mackenzie J, Huang Q, Iwamoto TJ. *Sol-Gel Sci and Tech* 1996;7:151.
- [43] Vieth WR, Sladek KJ. *J Colloid Sci* 1965;20:1014.
- [44] Stevens NSM, Rezac ME. *Chem Eng Sci* 1998;53:1699.